INSTABILITY OF THE ROTATING GRAVITY FLOW DOWN A SLOPE

Honji, Hiroyuki
Research Institute for Applied Mechanics, Kyushu University : Professor

Hosoyamada, Tokuzo
Department of Civil Engineering Hydraulics and Soil Mechanics, Kyushu University : Postgr., Dep

https://doi.org/10.5109/6781084

出版情報：Reports of Research Institute for Applied Mechanics. 35 (105), pp.55-64, 1989-02. 九州大学応用力学研究所

Note

Reports of Research Institute for Applied Mechanics
Vol. XXXV, No. 105, 1989

INSTABILITY OF THE ROTATING GRAVITY FLOW DOWN A SLOPE

By Hiroyuki HONJI* and Tokuzo HOSOYAMADA**

A three-dimensional instability of the two-dimensionally induced, rotating, gravity flow down a 34° slope has been investigated experimentally using the electrolytic precipitation method of flow visualization. The instability is governed by ρ', the non-dimensional density difference between gravity-flow and ambient waters, and Ta, the Taylor number. A regular, three-dimensional, instability structure forms in the flow on the sloping bottom floor at $0.65 < \rho' < 3.5$ and $3.0 \times 10^3 < \mathrm{Ta} < 1.8 \times 10^4$.

Key words: Gravity flow, Rotating flow, Flow visualization

1. Introduction

The structure and dynamics of gravity flows generated by a density difference between flowing and ambient fluids have been investigated in diverse disciplines of physical sciences and engineering[1]. Gravity flows occur commonly in natural environments, and their spatial and temporal scales are smaller as compared with those of the global atmospheric and oceanic circulations. Relatively few papers, therefore, have been concerned with the gravity flows of dense fluids under the effect of the earth's rotation. However, some gravity flows such as turbidity currents on a continental slope and the deep-sea currents of dense water mass can be affected by the earth's rotation.

This paper reports some laboratory results which have relevance to the rotation effect on the structure of a thermally-induced gravity flow down a sloping, plane, bottom floor in a rotating water tank.

* Prof., Res. Inst. Appl. Mech., Kyushu Univ., Kasuga 816, Jpn.
** Postgr., Dept. Hydr. Civil Eng., Kyushu Univ., Fukuoka 812, Jpn.

2. Experemental methods

Experiments were carried out using a square water tank made of transparent Perspex plates. The experimental set-up is illustrated schematically in Fig. 1. The tank having the dimensions of 75×30×15 cm was put on a turntable with

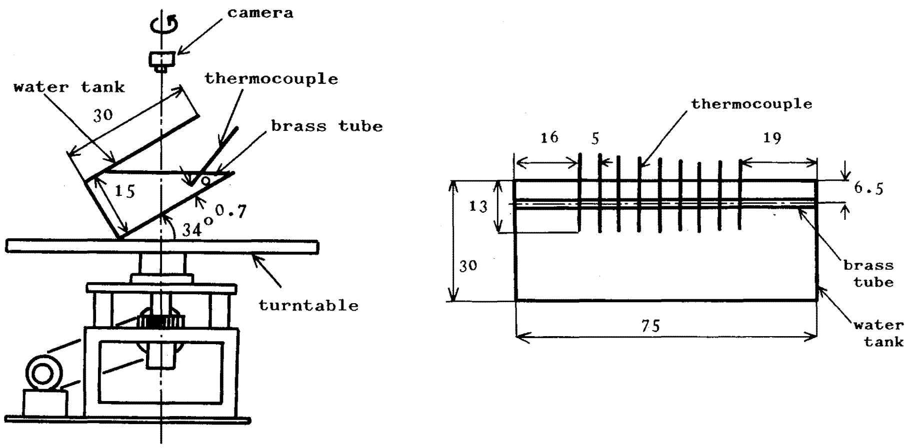

Fig. 1 Experimental apparatus (Dimensions in cm): (a) Side view, (b) Top view

a sloping angle of 34° from the horizontal. The tank was filled with tap water up to a level at which the water began to overflow the lower edge of the tank wall. The inside surface of the lower tank wall worked as a sloping bottom floor along which a heavier fluid flowed down continuously.

The heavier dense fluid was generated by cooling the ambient water surrounding a brass tube, through which a cold water was forced to circulate fast by means of a motor-driven constant-temperature reservoir of water. The cooling tube was 73 cm in length, and 10 mm and 8 mm in outside and inside diameters, repectively. The water reservoir system was also mounted on the turntable. The cooling tube lay, with its axis horizontal, on the near-top inside surface of the lower tank wall. The generated dense fluid flowed down along the sloping floor slowly. The flow remained stable and two-dimensional at small angular velocities of the system (ω) and became three-dimensional at larger ω.

The turntable on which the tank system was placed has the diameter of 1 m, and can be rotated in the counterclockwise direction at $\omega < 1.1\ s^{-1}$. The electrolytic precipitation method of flow visualization was used mainly[2]. A smoke-generating solder strip was fixed to the surface of the cooling tube. A low d. c. voltage was applied between the strip and a cathode in the tank to produce white dye smoke as a tracer. The aluminum flake method was also used partly. A 0.7 cm -thick parallel-to-floor water layer above the floor surface was illuminated for photographing flow patterns.

Water temperatures in the gravity flow were measured at every one minute with a temperature logger with 9 thermocouples lying on the bottom floor as shown in Fig. 1(b). The temperature resolution was 0.1°C.

A comment should be made on the effect of three narrow side walls of the tank. The size of the turntable limited that of the tank, and the flow patterns in the tank were unavoidably affected by these walls. Attention was, therefore, focused only on the flow patterns near the cooling tube rather than the overall ones.

The following experimental procedure was taken: After the steady rotation of the system was reached the gravity flow generation was started at time $t = 0$ s. Steady-flow observations were made after the flow became almost steady; t multiplied by the gravity fluid viscosity and divided by the square of the tube diameter ranged from 9 to 14, beyond which the flow began to be contaminated by the dense-water mass sedimented at the bottom corner of the tank and to be inactive due to a long-time thermal diffusion in the cooling reservoir water.

3. Results and discussion

The gravity flow patterns are shown in the series of photographs under Fig. 2 at different values of ρ' and Ta. The non-dimensional density difference ρ' is defined as

$$\rho' = g\Delta\rho/4\rho\omega^2 D, \qquad (1)$$

where g is the acceleration due to gravity, $\Delta\rho$ the density difference between the dense water near the tube and the ambient water, ρ the density of ambient water, and D the outside diameter of the cooling tube. The Taylor number is defined as

$$Ta = 4\omega^2 D^4/\nu^2, \qquad (2)$$

where ν is the kinematic viscosity of the water in the gravity flows. These figures show the flows viewed from top of the tank. The cooling brass tube emanating white smoke will be seen lying horizontally in an upper part of each photograph. The direction of rotation of the system is always counterclockwise.

In Fig. 2 the flow patterns are arranged in the order of increasing ω. Fig. 2(a) shows a basically structureless, two-dimensional, stable gravity flow in a non-rotating system. The flow in this case consists of a sheet of dense water originally generated around the tube. Although fine streaks of the smoke formed due to some roughness of the tube surface are seen in the sheet, these are inessential to interpretation of the flow.

Figure 2(b) shows a gravity flow consisting of a plane sheet of dense water and several thick streaks in it. The flow steers to the left due to the Coriolis

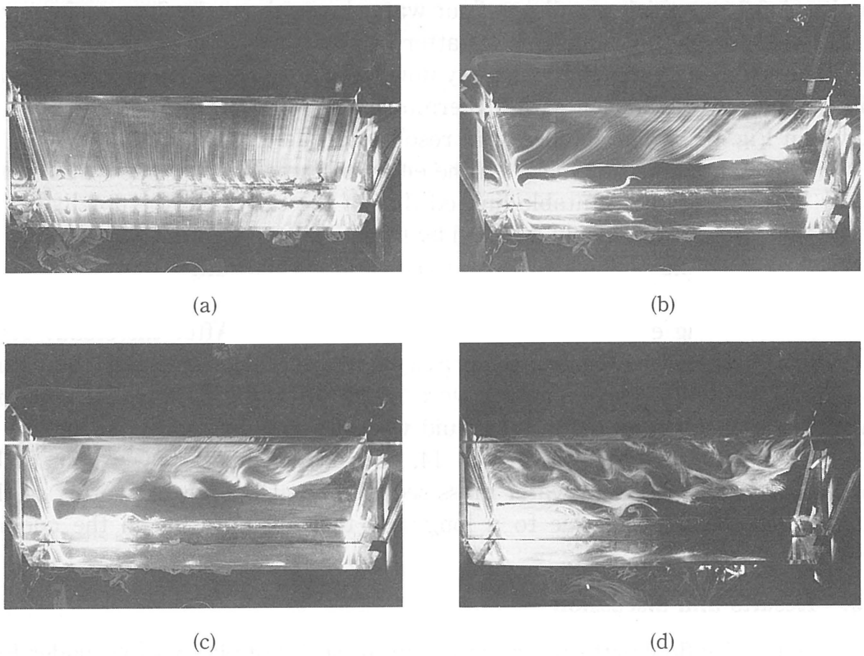

Fig. 2 Variation of rotating gravity flows with ρ' and Ta at $\Delta\rho/\rho \simeq 2.2\times10^{-3}$ and $t \simeq 12$ min (except for (d))
(a) $\rho' = \infty$, $Ta = 0$, $\omega = 0\ s^{-1}$
(b) $\rho' = 5.36$, $Ta = 2.07\times10^3$, $\omega = 0.31\ s^{-1}$
(c) $\rho' = 2.78$, $Ta = 3.67\times10^3$, $\omega = 0.44\ s^{-1}$
(d) $\rho' = 1.64$, $Ta = 6.94\times10^3$, $\omega = 0.56\ s^{-1}$, $t \simeq 16$ min

force as it goes downward. The figure shows the beginning of an instability, although mostly the flow is still two-dimensional.

As ω increases the above-mentioned streaks disappear and instead a wavy pattern of the flow appears as shown in Fig. 2(c). Note that this is not actually a propagatory wave but just a wave-like instability. The flow is three-dimensional. As ω increases further, the wavy pattern becomes more pronounced and the thick oblique streaks arrange themselves nearly equidistantly on the bottom floor as shown in Fig. 2(d). Note that these streaks slanted to the right are different from those shown in Fig. 2(b). Figure 2(d) shows a typical regular three-dimensional instability structure in the gravity flow down the slope. From these results it may be concluded that the upper critical value of ρ' for the formation of the regular, three-dimensional, instability structure is around 3.5.

Figure 3(a～c) shows the time -wise variation of a gravity flow at later stages of its development, when ρ' is further decreased (Ta is further increased).

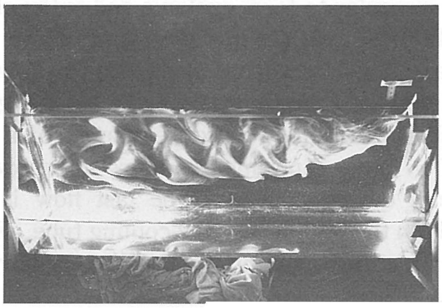

(a)

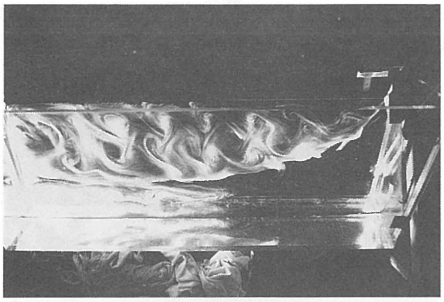

(b)

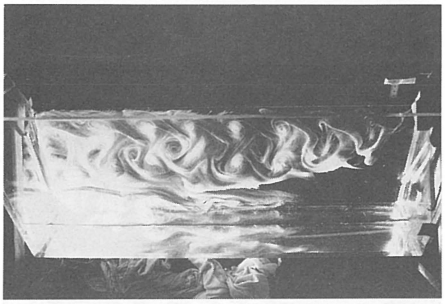

(c)

Fig. 3 Development of rotating gravity flow at $\rho' = 0.770$ and $Ta = 1.23\times10^4$, $\Delta\rho/\rho = 1.3\times10^{-3}$ and $\omega = 0.64\ \mathrm{s}^{-1}$

(a) $t = 13$ min 55 s

(b) $t = 15$ min 10 s

(c) $t = 16$ min 8 s

Dye streaks become irregular to form cyclonic and anticyclonic vortices as time goes on. As a whole these vortices make up a structure which reminds us of Kārmān's vortex trail. The lower front of the gravity flow is slanted to the left and each thick dye streak to the right, similarly as in Fig. 2.

Figure 4(a, b) shows the time-wise development of a gravity flow for the smallest ρ' (largest Ta) in the experiment. Figure 4(a) shows the developing flow and Fig. 4(b) the fully developed one. The last flow is quite irregular and turbulent particularly in the region near the cooling tube. From Figs. 3 and 4 the lower critical value of ρ' for the formation of the regular instability structure may be around 0.65.

All the flow patterns shown above were visualized with dye smoke generated by means of the electrolytic precipitation method. What is visualized with this method is actually the so called 'integrated streaksheet' somewhat different from common fluid-mechanical lines[3]. Therefore, it would be desirable to visualize the flow by using some common method. Figure 5 shows an example

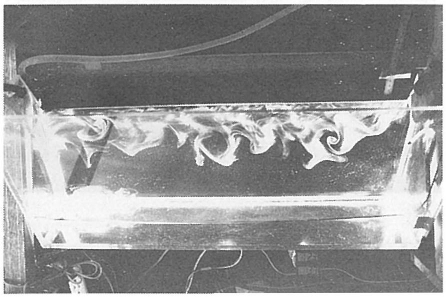

(a)

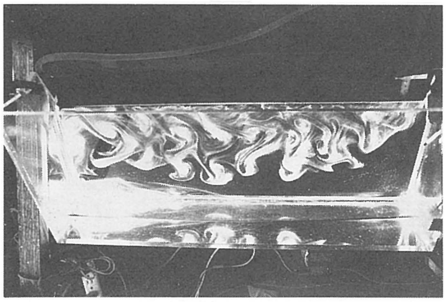

(b)

Fig. 4 Development of rotating gravity flow at small $\rho' = 0.502$; $Ta = 2.37\times10^4$, $\Delta\rho/\rho = 2.5\times10^{-3}$, $\omega = 1.10\ s^{-1}$

(a) $t = 11$ min 43 s

(b) $t = 12$ min 47 s

of flow pattern vinualized with suspended aluminum flakes. A similar, wavy, instability structure is seen in the flow, although it is not much clear as compared with the smoke flow patterns.

A vertical cross-sectional view of a gravity flow near the center of the tank is shown in Fig. 6(a), and illustrated schematically in Fig. 6(b). The flow is visualized with aluminum flakes in combination with dye smoke. The region of the gravity flow is confined to a thin layer on the sloping floor, and almost no motion of suspended flakes is perceptible in the remaining region of ambient water.

The gravity flows have been generated two-dimensionally by cooling the water surrounding the straight brass tube. Therefore, the lateral distribution of water temperature in the gravity flows is anticipated to someway reflect the instability structure. The temperature profiles at three values of ρ' are shown in Fig. 7(a∼c), in which X is the distance measured from the left side wall of the tank laterally along its horizontal long axis (Fig. 1). The temperature profile is rather flat and no structure is indicated in Fig. 7(a) at large ρ' and small Ta. As ρ' is decreased and Ta increased, the temperature profiles connecting through the data taken at larger t clearly reflect the instability structure of the flow as depicted in Figs. 7(b) and (c).

The region of formation of the regular, three-dimensional, instability structure is summarized in Fig. 8, based on the results of photographic observations. Due to technical limitations in the experiment, the data points lie nearly on a straight line in the log-log diagram. The region in the middle of Fig. 8 for the regular structure ranges approximately from 0.65 to 3.5 in ρ', and from 3.0×10^3 to 1.8×10^4 in Ta. The flow remains stable and two-dimensional in the upper left region, and becomes irregular and turbulent in the lower right region in the figure.

Flow regime diagrams of the type shown above are commonly used for summarizing laboratory results on rotaing stratified flows, and their overall interior fields associated with baroclinic instability are usually the center of interest. In the present case, however, the flow occurs mainly on the bottom floor and no conspicuous motion of the interior water mass takes place. The cause for the formation of the instability structure in the gravity flow, therefore, still remains open and further investigations on the characteristics of the flow are needed to clarify the formation mechanism.

Acknowledgments

This work was supported by a Ministry of Education grant for the Priority Area Research Programme 'Dynamics of the Deep Ocean Circulation', which is gratefully acknowledged. We would like to experess our sincere thanks to Professors T. Teramoto, Y. Nagata, K. Taira, and R. Kimura for their valuable discussions and encouragement throughout this experiment.

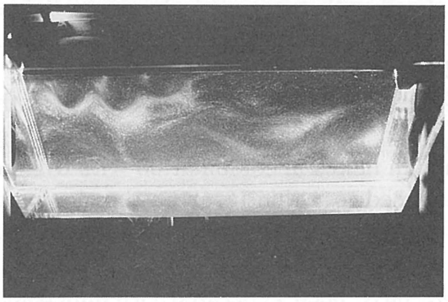

Fig. 5 Rotating gravity flow visualized with suspended aluminum flakes at $\omega = 0.62\ s^{-1}$; $\rho' = 1.68$, $Ta = 1.00 \times 10^4$, $\Delta\rho/\rho = 2.6 \times 10^{-3}$, $t \simeq 16$ min

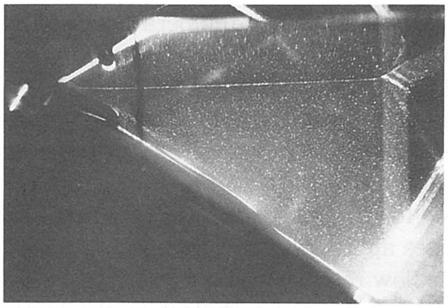

(a)

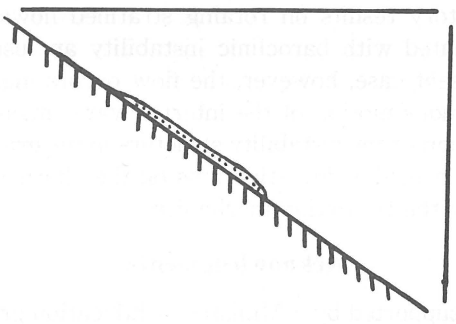

(b)

Fig. 6 Side view of rotating gravity flow
(a) $\rho' = 1.27$, $Ta = 1.00 \times 10^4$, $\Delta\rho/\rho = 2.2 \times 10^{-3}$, $\omega = 0.65\ s^{-1}$, $t = 3$ min 23 s
(b) Schematic diagram

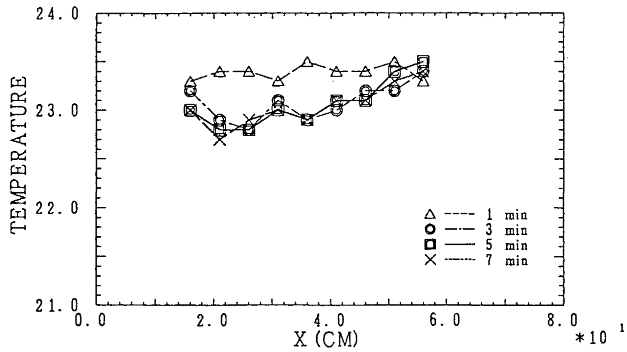

(a)

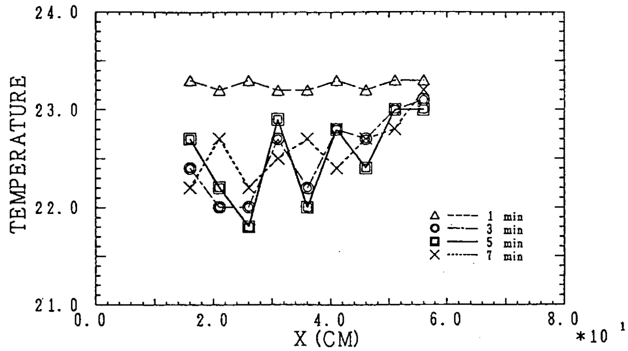

(b)

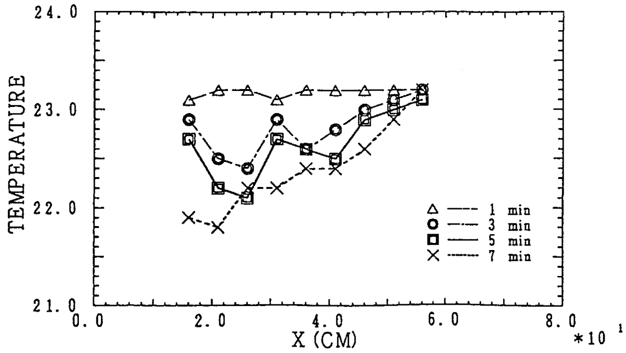

(c)

Fig. 7 Water temperature °C distributions in rotating gravity flows at $\Delta\rho/\rho = 2.3\times10^{-3}$ with times (t) shown in each figure

(a) $\rho' = 5.02$, $Ta = 2.77\times10^3$, $\omega = 0.33\ \mathrm{s}^{-1}$

(b) $\rho' = 1.41$, $Ta = 9.07\times10^3$, $\omega = 0.65\ \mathrm{s}^{-1}$

(c) $\rho' = 1.31$, $Ta = 9.07\times10^3$, $\omega = 0.66\ \mathrm{s}^{-1}$

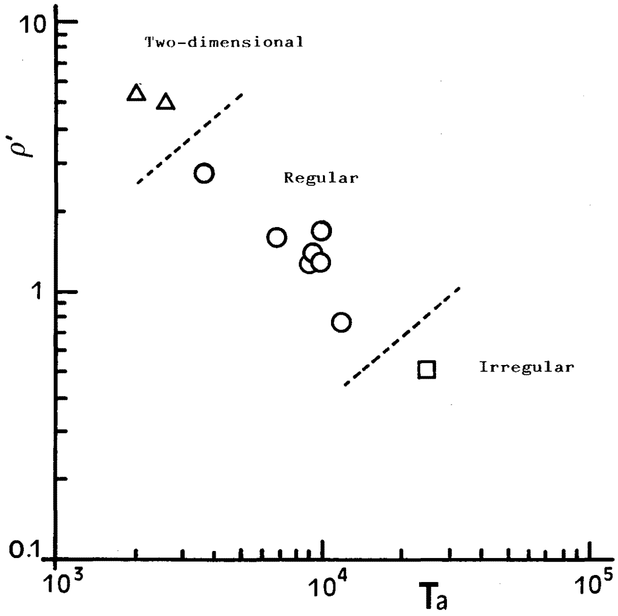

Fig. 8 Regime diagram for the rotating gravity flow down the 34° slope

References

1) Simpson, J. E.: *Gravity Currents: In the Environment and the Laboratory*, Ellis Horwood Ltd., Chichester, 1987.
2) Donnelly, R. J.: Fluid Dynamics (In: *Physics Vade Mecum*, ed. H. L. Anderson), Amer. Inst. Phys. 1981, N. Y., p. 193.
3) Honji, H.: Streaked flow around an oscillating circular cylinder, J. Fluid Mech. **107** (1981) 509-520.

(Received December 3, 1988)